Validation testing of a peridynamic impact damage model using NASA's Micro-Particle Gun

Forrest E. Baber[a], Brian J. Zelinski*[b], Ibrahim Guven[a], Perry Gray[c]

[a]Virginia Commonwealth University, Richmond, VA USA 23284; [b]Raytheon Missile Systems, Tucson, AZ USA 85706; [c]NASA/Marshall Space Flight Center, AL USA 35812

ABSTRACT

Through a collaborative effort between the Virginia Commonwealth University and Raytheon, a peridynamic model for sand impact damage has been developed[1-3]. Model development has focused on simulating impacts of sand particles on ZnS traveling at velocities consistent with aircraft take-off and landing speeds. The model reproduces common features of impact damage including pit and radial cracks, and, under some conditions, lateral cracks. This study focuses on a preliminary validation exercise in which simulation results from the peridynamic model are compared to a limited experimental data set generated by NASA's recently developed micro-particle gun (MPG). The MPG facility measures the dimensions and incoming and rebound velocities of the impact particles. It also links each particle to a specific impact site and its associated damage. In this validation exercise parameters of the peridynamic model are adjusted to fit the experimentally observed pit diameter, average length of radial cracks and rebound velocities for 4 impacts of 300 μm glass beads on ZnS. Results indicate that a reasonable fit of these impact characteristics can be obtained by suitable adjustment of the peridynamic input parameters, demonstrating that the MPG can be used effectively as a validation tool for impact modeling and that the peridynamic sand impact model described herein possesses not only a qualitative but also a quantitative ability to simulate sand impact events.

Keywords: sand erosion, impact damage, peridynamic simulation, ZnS, radial crack, lateral crack, infrared sensor, micro-particle gun

1. INTRODUCTION

Sand particle impacts at high speeds can cause considerable damage to optical aperture materials. In order to understand the nature of this damage and to develop effective strategies for its mitigation a peridynamic model has been developed. The model has been exercised to simulate damage caused by sand impacts on aircraft instrument windows under take-off, landing, and low altitude cruise conditions. Typical impact conditions include sand particles with diameters on the order of 150 microns at flight speeds of 75 m/s or higher. Impacts under these conditions can cause small pits, cracks, and subsurface damage in aperture materials which scatter or block incoming light, leading to reduced transmission. Aperture materials which must pass long-wavelength infrared radiation (LWIR), such as zinc sulfide, ZnS, are particularly prone to transmission erosion from sand impacts because they are weaker and softer than aperture materials commonly used for mid-wavelength infrared radiation (MWIR) applications.

Early results from the peridynamic model of sand impact damage demonstrated its ability to simulate the phenomenological characteristics of impact damage, including pit formation, radial cracking, and lateral cracking[1]. In addition, an accompanying peridynamic model of a Vickers indentation test was developed and used to extract the input parameters needed to run the sand impact model from experimental data. A second paper described improvements in the fidelity of the simulation achieved by modifying the mechanical properties of the simulation impactors to more closely resemble that of quartz sand and documented the large variability in damage characteristics observed as a function of the shape of the impactor[2]. The versatility of the peridynamic model was demonstrated in a third paper, which described the effects of coatings, substrate properties, incident angle, and tilt on the resulting damage[3].

A key finding of the second study was that lateral cracks only form when the impacting face is relatively flat. Rounded and sharp tipped impact surfaces did not cause lateral cracking. This result is consistent with experimental observations, which show a wide variability in the size of damage caused by sand particle impacts in ZnS, for example. Standardized testing of sand erosion resistance is often conducted by blasting a test surface with a known quantity and size distribution

---

*BZelinski@Raytheon.com; phone 1-520-794-2592

of sand particles at a given velocity. However, the particles used in tests such as these are not regularly shaped; nor do they have well-defined flat surfaces (see Figure 1). As a result, the large variability of sand particle shape and size, the inability to control the orientation of the particles during impact, and the sensitivity of the extent of damage to the geometry and flatness of the impacting surface (as revealed by simulations) make validation testing of the peridynamic impact model using sand blasting approaches extremely difficult. So, while the current model has provided considerable insight into sand impact phenomenology, and provides quantitative data regarding damage extents for given impact conditions, it remains to be fully vetted by validation testing.
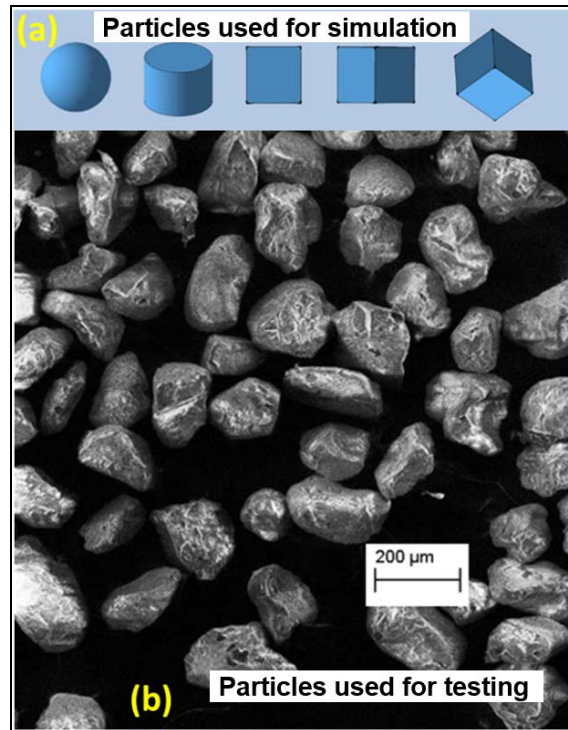

Figure 1. Composite of impactor shapes and sizes used to simulate sand impact damage in peridynamic model (a), and sand particles used for standard sand erosion testing (b). The 200 μm bar applies to both images. Note the lack of regularity in both size and shape of the sand particles. All particles ostensibly have the same mass as a spherical particle having the density of quartz and a diameter of 160 μm.

Recently, Perry Gray, at the NASA Marshall Space Flight Center, developed a new technique for accelerating a small quantity of particles at a substrate, recording the resulting impacts, and simultaneously measuring the incoming and rebound velocities of the particles. This paper describes the use of this technique to conduct a preliminary assessment of the validity of the peridynamic sand impact model. The use of spherical particles, combined with the ability to characterize the relevant velocities of the impact event eliminate all of the ambiguities described above associated with the use of the sand blasting approach for validation testing.

2. TEST APPARATUS

Precise control and monitoring of impact conditions is achieved in the micro-particle gun by the use of a reproducible launching mechanism and a set of high speed cameras. The heart of the test apparatus developed by Gray consists of a plastic piston whose top surface contains a dimple filled by the impacting particles. The piston is accelerated upwards through a barrel by compressed helium gas until it is stopped by a bulkhead containing a hole, through which the particles continue to travel. The particles then impact the surface of the substrate under study while a camera, located at the top, images down through the substrate to capture the location and characteristics of the impact sites. At the same time a side camera captures the impact events, recording the positions of all the particles just prior to and after impact.

Vertically and horizontally mounted strobes, timed to flash at impact, provide the illumination needed to enable imaging by the cameras (see Figure 2).
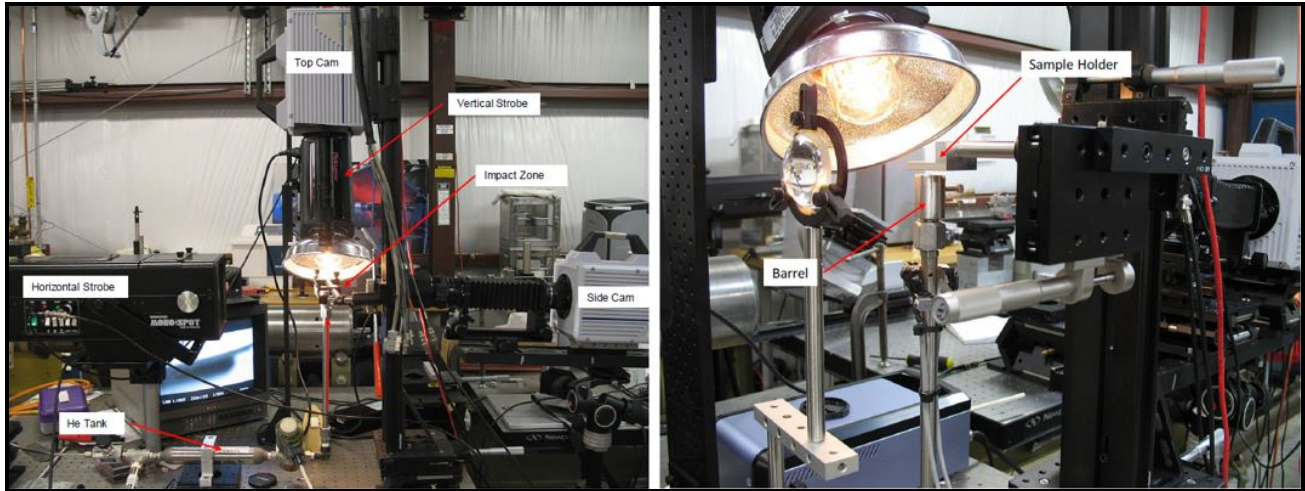

Figure 2. Micro-particle gun setup and component identification (left), close-up of barrel and sample holder (right).

Impact site and location imaging is achieved using a Photron SA 1.1 high speed video camera run at 125,000 frames/s (8 µs). At this rate the camera can run for several seconds and record all impact events with a resolution of 128 X 256 pixels. A Shimadzu HPV-2 camera images the impact events from the side. The HPV-2 has a fixed resolution of 260 X 312 at all frame rates and a frame rate capability of 1,000,000 frames/s (1µs). The main limitation of this camera is that it can only record approximately 100 frames of data. This limits run times and increases the chance that some of the impacts will not be recorded. However, this fast frame rate is needed to capture multiple locations of the incoming and rebounding particles in order to calculate velocities when impact speeds exceed 100 m/s.

The barrel is constructed such that the impact sites from a single multi-particle shot are grouped in a circle with a diameter of only 2 mm. This tight grouping enables multiple shots to be conducted on a single 1 inch substrate. A grid with a spacing of 5 mm is drawn and registered on the sample so as to track the results from multiple trials of the gun. In a single shot the particles strike the substrate with different velocities as a result of interactions with the gun barrel and with each other during launch and flight. The spreading of the velocities is fortuitous in that considerable information about the velocity dependence of damage can be extracted from a single shot (as is done in this study).

3. EXPERIMENTAL DATA REDUCTION

An example of the type of data generated by the micro-particle gun for glass beads impacting a ZnS substrate is shown in Figure 3.
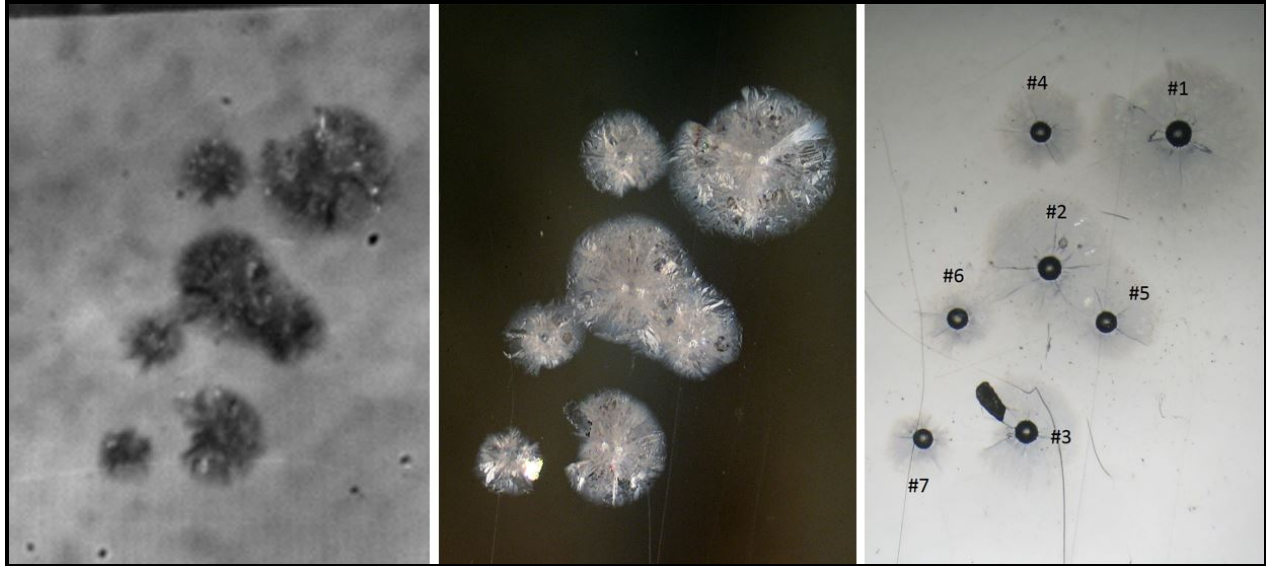
Figure 3. Damage generated on a ZnS substrate by a single shot of the micro-particle gun as imaged by the Photron camera (left), optical microscopy illuminated by light from the side (middle) and by transmitted light (right).

The left image in Figure 3 shows the image captured by the Photron camera after impact of the particles from a single shot. An image corresponding to the same sample location is shown in the middle figure as captured by optical microscopy using side illumination. Illumination from the side highlights the subsurface damage, including lateral cracking, caused by the particle impacts. The image on the right shows the damage as illuminated by transmitted light in the optical microscope, the viewing conditions which emphasize pit formation from the glass bead impacts. The impacts in this image on the right are numbered in the order of decreasing velocity of impact.

In order to correlate damage sites with particles of a known diameter and velocity, images from the Photron and Shimadzu cameras are correlated. Figure 4 shows a portion of two frames from the Photron camera data taken of the glass bead and the damage it caused as site #4, shown in Figure 3, was generated. Larger portions of the frame (see Figure 3, left) capture the spatial relationships between impact sites and allow for identification and linkage of specific particles with the damage they generate. Using time sequencing data, the images from the Shimadzu cameras are inspected to isolate the impact event for a given particle and then analyzed to calculate the distance the particle travels between successive frames, both prior to and after impact, to determine incoming and rebound velocities.
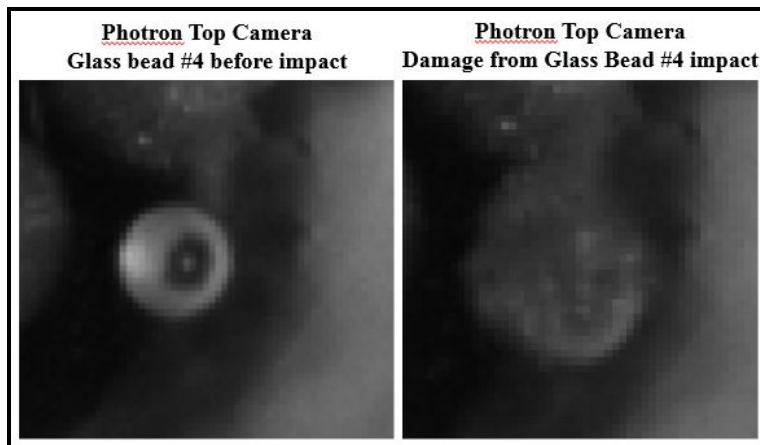

Figure 4. Photron images of the glass bead just prior to impact (left) and the resulting damage, labelled site #4 (right).

For example, Figure 5 shows two images which allow calculation of the rebound velocity for impact #4. Note that each image contains a reflection of the scene with the substrate acting as the mirror plane. The left image in the figure shows the particle just after the impact has taken place, as the damage pit is clearly visible. The right hand image captures the location of the particle at some moment after impact. The distance the particle travels between frames times the frame rate results in a quantitative measure of the velocity.
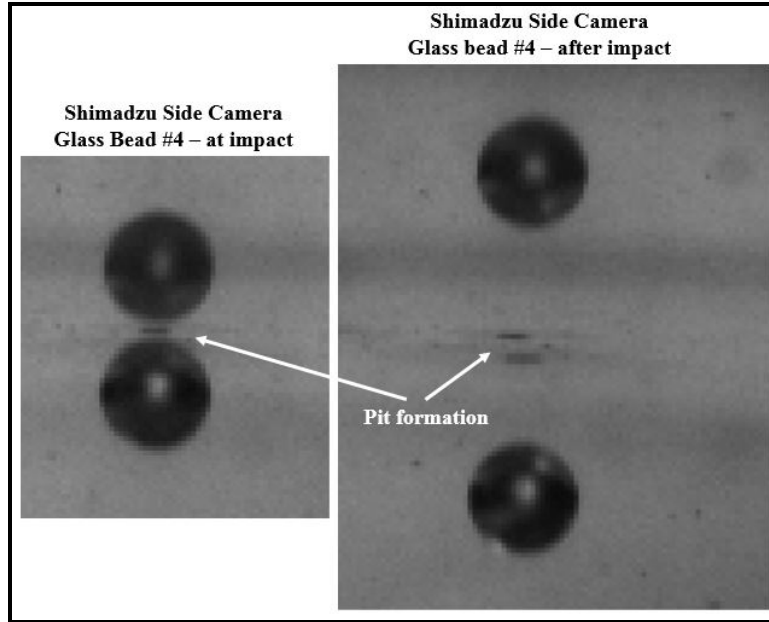

Figure 5. Schimadzu images of the glass bead just after impact (left) and one frame later for damage site #4 (right).

4. EXPERIMENTAL DATA

The specific data analyzed in this report were obtained from two shots of the micro-particle gun firing 300 μm diameter soda lime silicate glass beads at a multi-spectral ZnS substrate (Cleartran®). The impact damage and the resulting data analysis from the first shot is shown in Figure 6.
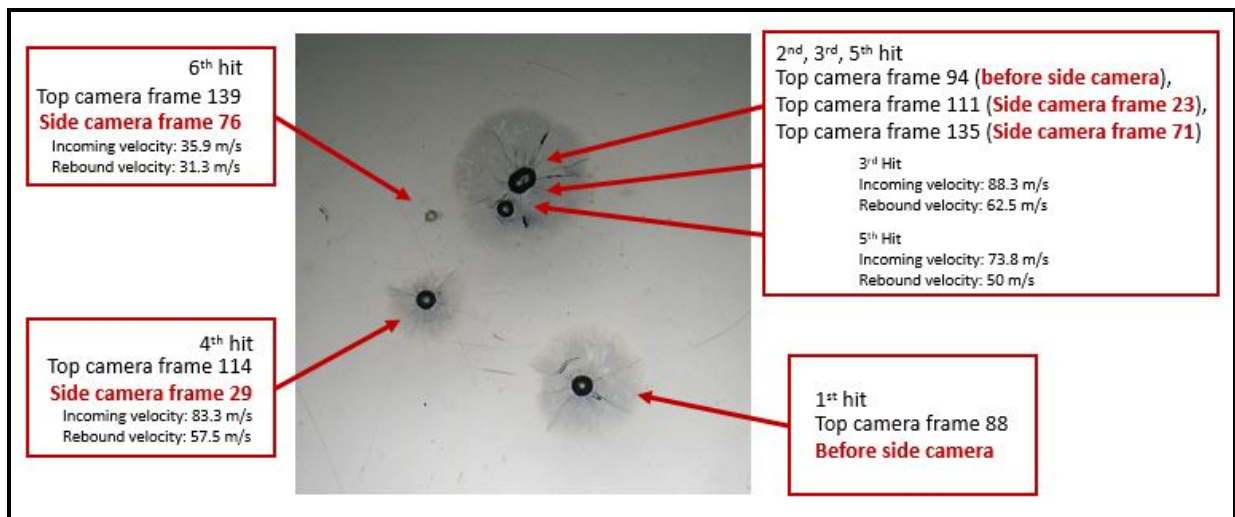

Figure 6. Optical microscope image of damage from shot 1 with data assignments for each impact.

Although the optical image of the damage does not obviously indicate, this shot produced 6 impacts from glass beads. The 2nd, 3rd, and 5th impacts took place very close to each other spatially, with the pits from impacts 2 and 3 overlapping. As noted earlier, there is some variability in the velocity of the particles in a single shot resulting in some spread in their arrival times at the substrate. This leads to the situation that some of the impact events are not recorded by both the top and side cameras. The 1st impact took place before the side camera was triggered, thus velocity data cannot be extracted for this event. The same is true for the 2nd impact. Because the 3rd impact overlaps with the 5th, only velocity data will be used in the following analysis. The damage caused by these two impacts overlaps and so cannot be uambiguously characterized for comparison to the peridynamic modeling results. Consequently, the 1st shot produced two clean and complete data sets for the validation exercise, from the 4th and 6th impacts.

The data reduction for impacts #4 and #6 of shot 1 is illustrated in Figure 7. Here the distances for all observable radial cracks, as well as the diameter of the impact pits are measured using image analysis software on the optical microscope and the average radial crack length is calculated for comparison with the simulation results. The length of any one radial crack is taken as the distance from the edge of the rim to the end of the crack.
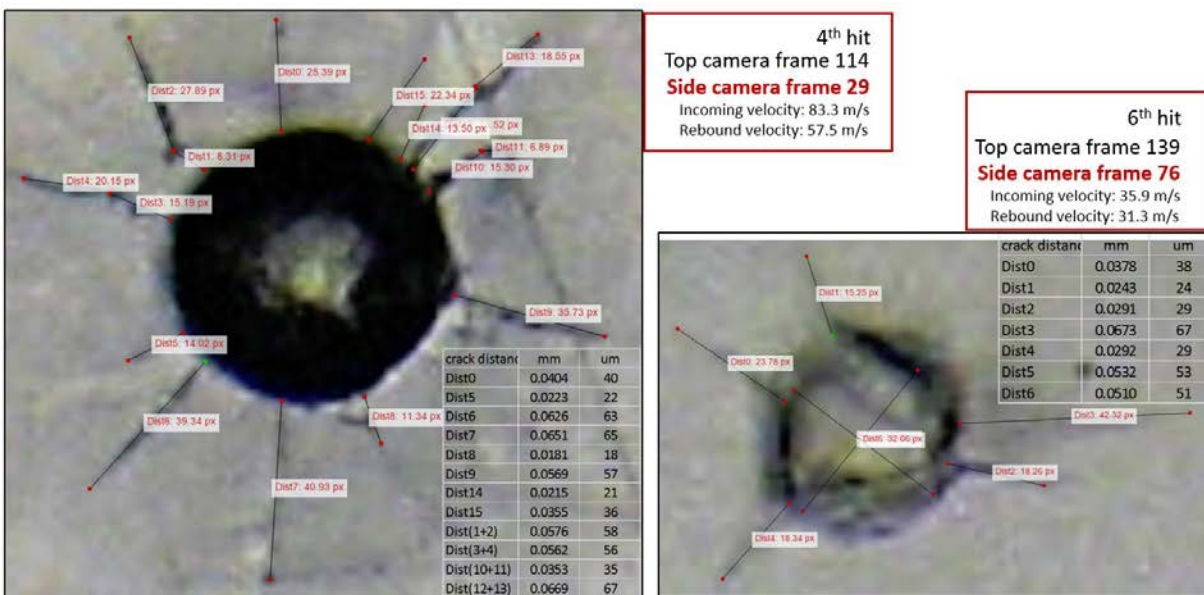

Figure 7. Data reduction for impacts #4 and #6 of shot 1.

The second shot, Figure 8, produced two impacts which are included in this preliminary validation exercise, the 3rd and 4th impacts. Six impacts are visible in the optical image, however the impact velocities and spread of the particle impact sites varied sufficiently such that complete data sets were not available for the other 4 impacts. For completeness, the data reduction from the second shot is shown in Figure 9. In both shots 1 and 2, the data included impacts caused by particles which hit the substrate, bounced back, reflected off the end of the barrel and hit the substrate a second time. Multiple bounces reduce the velocity of the particle and broaden the spectrum of velocities which can be accessed in a single shot. In shot 1, hit #6 was one such "reflected" particle, as was hit #2 in shot 2.
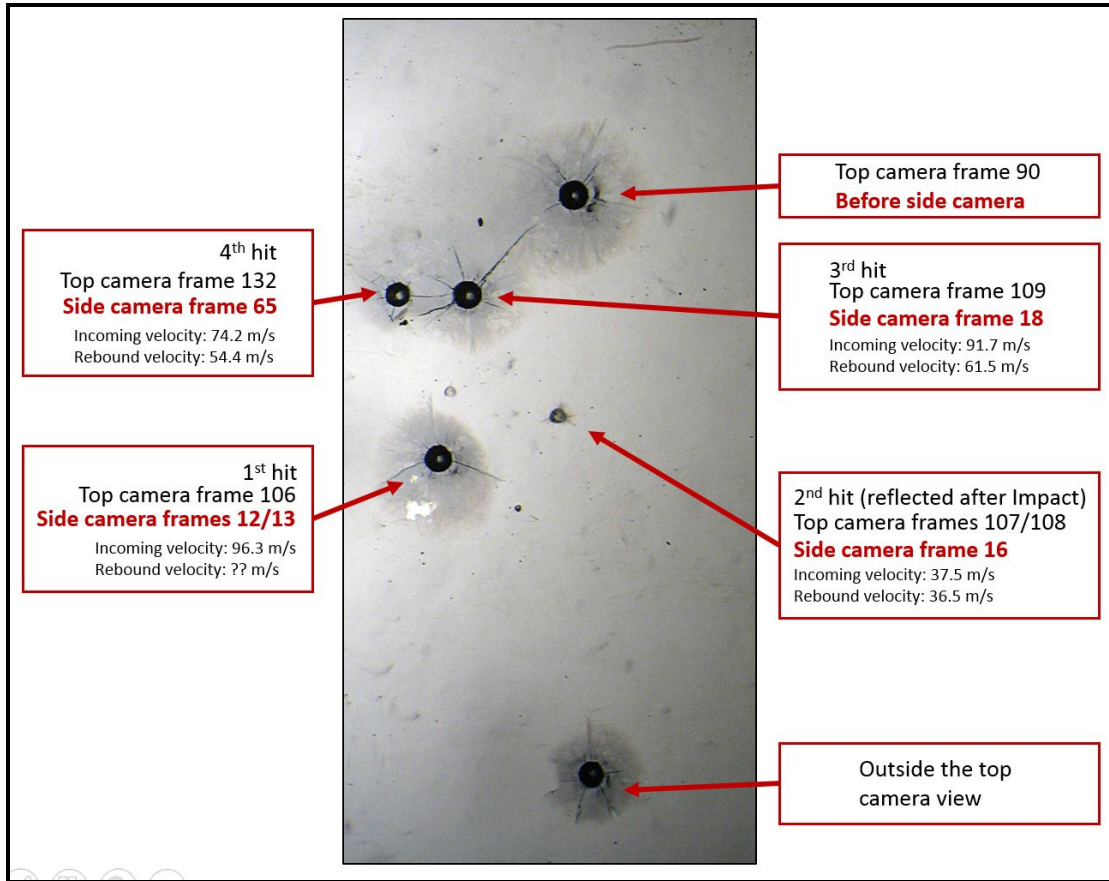
Figure 8. Optical microscope image of damage from shot 2 with data assignments for each impact.
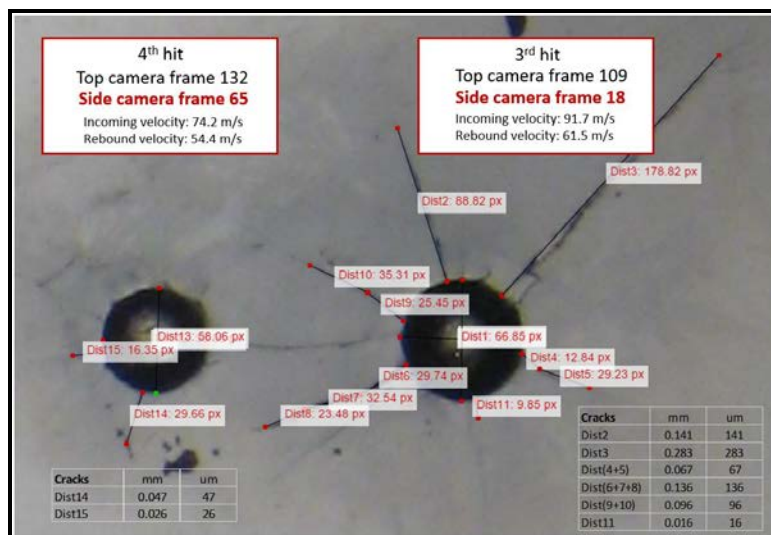

Figure 9. Data reduction for impacts #3 and #4 of shot 2.

5. PERIDYNAMIC SIMULATION METHOD

Details of peridynamic theory and its application to sand impact phenomenology have been described previously[1]. In short, the theory reformulates the mathematical foundations of solid mechanics such that differentiations with respect to spatial coordinates are avoided. Instead, the governing equations of mechanics are expressed as integral equations, and so undefined conditions do not arise at interfaces and crack surfaces. Stress and strain do not appear in the governing equations and stretch and force fields present between material points drive the deformation behavior. Material failure is readily incorporated in the formulation, leading to a natural definition of a damage field. As a result, fracture initiation and propagation are simulated without the need for extrinsic kinetic models of crack formation.

In this study the peridynamic model simulated the impact of spherical glass beads with multi-spectral ZnS. The glass beads had the mechanical properties of soda-lime silicate glass, diameters of 300 μm and incoming velocities of 83.3 m/s, 35.9 m/s, 91.7 m/s and 74.2 m/s. These velocities were chosen to match the velocities observed during the experimental measurements. The simulated substrate possessed a diameter of 600 μm and thickness of 300 um and was constrained along the vertical edges to prevent horizontal motion. The top and bottom surfaces were free to move. The grid spacing for the peridynamic mesh was 8 μm for both the impactor and the substrate. In each simulation, the impactor was given the aforementioned initial velocity; shortly after the simulation begins, the impactor makes contact with the substrate surface and the simulation continues until damage propagation ceases.

6. SIMULATION RESULTS

In order to provide a preliminary assessment of the ability of micro-particle gun facility to provide validation data, the input parameters for ZnS, which characterize its mechanical response in the peridynamic sand impact model, were modified until a reasonable fit to the experimental data was obtained. An example of the type of data generated by the simulation is shown in Figure 10.
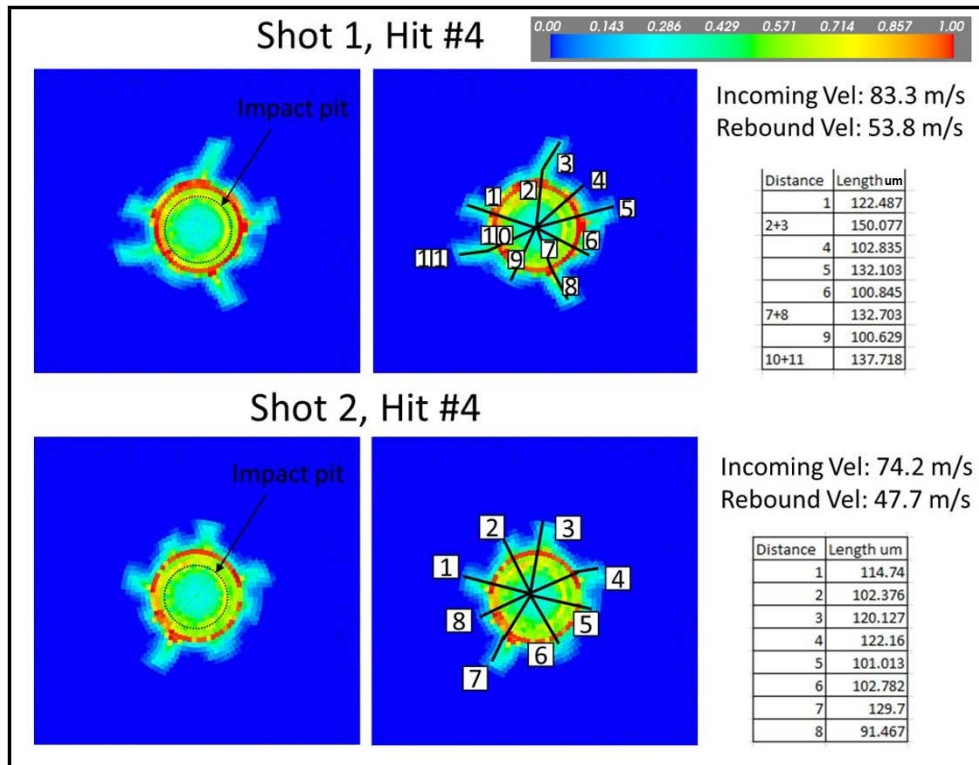

Figure 10. Portions of the surface of the ZnS substrate showing simulation results and measurements of defining characteristics of the damage from Shot 1-Hit #4 and Shot 2 – Hit #4.

As seen in Figure 10, the defining characteristics of the damage used for this validation exercise are the pit diameters and the radial crack lengths, the average of which are compared to the experimental equivalent. In this simulation a crack is defined as the collection of contiguous material points whose damage parameter equals 0.4. Recall that in peridynamics, the damage parameter is the ratio of the number of broken bonds between a material point and its neighbors in the simulation to the original number of bonds and ranges from 0 to 1. The length of the radial crack in the simulation is the distance from the material point located at or near the center of the damage and the material point farthest from the center which lies on both the surface of the substrate and the contiguous surface of the crack. The rim of the pit is defined in a similar fashion and the pit diameter is defined as the diameter of the best fit circle through the rim. To compare against the experimental data the length of the radial cracks from the simulation must first be reduced by the calculated pit radius, since the experimental data reports the rim to crack tip distance.

7. RESULTS OF VALIDATION EXERCISE

Using the experimental data from the 4 impacts of this study, the values of the critical stretch and yield strength of ZnS in the sand impact model were adjusted to achieve a reasonable fit with the average radial crack length and impact pit diameter. The resulting rebound velocity in the simulation was then compared to the experimental findings as a preliminary validation exercise. The results of this exercise are shown in Figures 11 and 12.
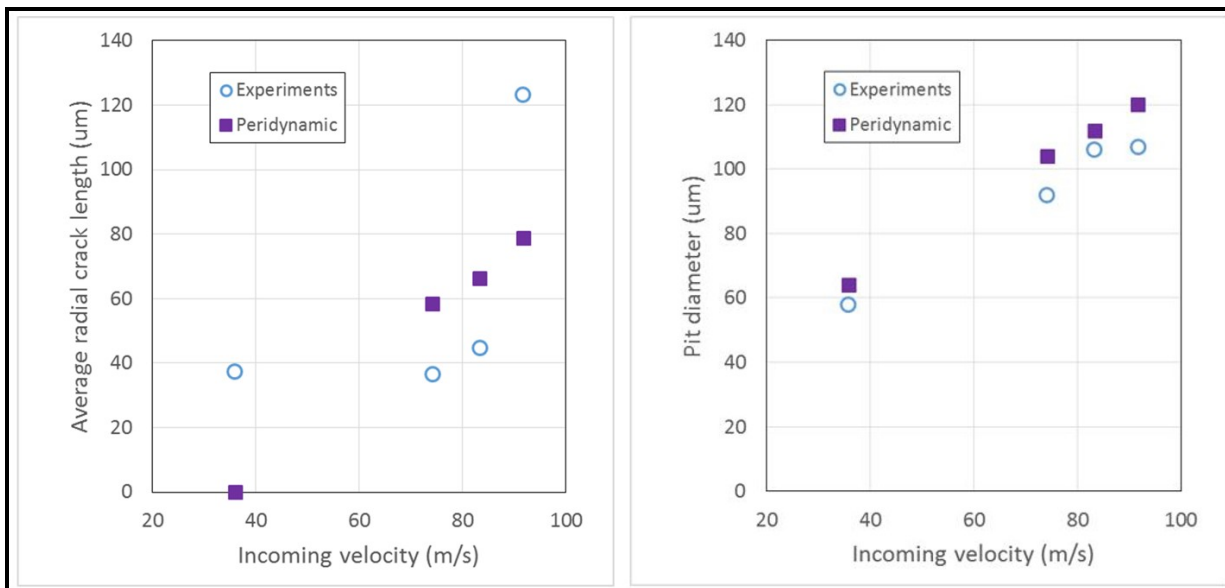

Figure 11. Average radial crack length and pit diameter as a function of the incoming velocity for 300 μm diameter glass bead impacts on ZnS.

As seen in Figure 11 (left) there was some spread in the experimental data for the average radial crack length. The peridynamic input parameters were adjusted so that the simulation results lay among the data for this parameter. The simulation results for the impact pit diameters exhibit the same velocity dependence and lay very close to the values obtained experimentally. In addition, the rebound velocity, as predicted by the peridynamic model, possesses a dependence on the incoming velocity which is similar to that of the experimental data, with the actual values being somewhat lower than measured from the micro-particle gun results.
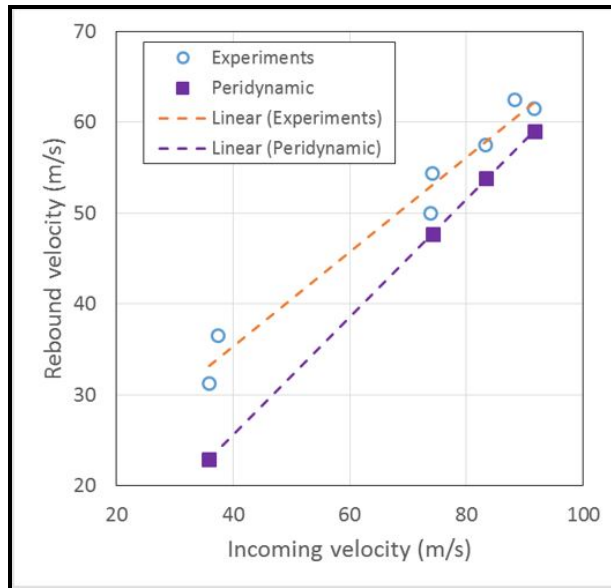
Figure 12. Rebound velocity versus incoming velocity for 300 μm diameter glass beads impacting ZnS.

8. DISCUSSION

As seen in Figures 11 and 12, reasonable agreement between the average radial crack length and pit diameters is achieved, including the proper rebound velocity dependence. These results are preliminary because only limited effort was made to optimize the fit. In particular, it was found that the modeled crack lengths were initially too long when the input parameters for critical stretch and yield strength used in all prior work (extracted from hardness indentation tests) were used. Changing the critical stretch from 0.0007 to 0.00092 (20% increase) led to the observed good agreement shown above for crack length.

However, after this adjustment, the rebound velocity was too low. In response, the yield strength was increased – this increased the rebound velocity (as more elastic energy could be stored in the substrate to return to the recoiling sphere), without significant effect on the crack and pit behavior to achieve the fit shown in Figure 11. Because of the limited nature of this data set, further efforts to improve the fit were not undertaken due to time constraints. It is likely that further increases in yield strength will improve the velocity match in Figure 12 without modifying the quality of the fit in Figure 11 significantly.

These results indicate than an interesting trade space exists between values of critical stretch, yield strength, and the physical damage and recoil effects for impact damage. This is the first time experimental data has been available to begin investigating trades between these parameters. Of equal interest is the implications with respect to the use of the optimized PD input parameters as obtained by the hardness indentation experimental fitting procedure. Further work should be done to examine the overlap in trade space and behavior between the impact results and the indentation model.

Overall the results above support the conclusion that the peridynamic model of sand impact damage has great potential to quantitatively capture the complex interactions and fracture behavior which take place during a sand impact. It also demonstrates that the MPG can be used effectively as a validation tool for impact modeling. More data will be gathered using the micro-particle gun to validate the peridynamic model, along with additional efforts to improve the quality of the fit using the larger data set to be obtained.

REFERENCES

[1] Guven, I. and Zelinski, B. J., "Peridynamic modeling of damage and fracture in EM windows and domes," Proc. SPIE 9453, 94530V SPIE Digital Library (2015).

[2] Schultz, R., Guven, I. and Zelinski, B. J., "Role of impactor properties on the computational simulation of particle impact damage in transparent ceramic windows," Proc. SPIE 9453, 94530O SPIE Digital Library (2015).

[3] Tune, S., Schultz, R., Guven, I. and Zelinski, B. J., "Peridynamic simulation of the effects of coatings, substrate properties, incident angle, and tilt on sand impact damage in transparent ceramic windows," Proc. SPIE 9453, 94530P SPIE Digital Library (2015).